DYNAMIC CONTROL OF GRAPHENE - ENABLED PLASMONIC NANOLASERS

Ho Xuan Truong[1*]

[1]*Dong Nai Technology University*

Corresponding author: Ho Xuan Truong, hoxuantruong@dntu.edu.vn*

GENERAL INFORMATION

Received date: 30/12/2023

Revised date: 05/02/2024

Published date: 12/03/2024

KEYWORD

Graphene Modulation;

Laser Miniaturization;

Opto-Electronic Integration;

Plasmonic Nanolasers;

Surface Plasmon Polaritons.

ABSTRACT

In this research, I have conceived and realized a pioneering development of a surface plasmon polariton nanolaser that harnesses graphene as its fundamental constituent. This unique nanolaser exhibits a distinctive feature: the ability to modulate its operation by applying an externally applied current while concurrently being optically stimulated. My investigation revolves around the innovative achievement of effectively switching the plasmonic nanolaser on and off for the very first time, making a milestone in the realm of nanophotonics. The utilization of graphene within the structural framework of the SPP nanolaser capitalizes on its extraordinary carrier mobility and remarkable electrical properties, thus rendering it an auspicious contender for integration into opto - electronic integrated circuits. This study presents a comprehensive exposition of experimental findings, illuminating the profound influence of graphene on the performance of plasmonic nanolasers, and delves into the underlying mechanistic intricacies.

1. INTRODUCTION

The relentless pursuit of miniaturization in laser technology, driven by the ever-expanding demands of modern photonics and integrated opto-electronic systems, has led to a profound evolution in laser design over the past few decades. A pivotal milestone in this journey was the advent of Vertical-Cavity Surface-Emitting Lasers (VCSELs) in the 1980s, which initiated a wave of innovation in laser miniaturization. Subsequently, novel laser architectures, such as microdisk lasers and nanowire lasers, emerged to further reduce cavity sizes and enhance performance (Xavier et al., 2018).

However, these advancements encountered a fundamental limitation imposed by the optical diffraction limit, which dictates that the mode volume of a resonant optical cavity should be at least $(\lambda/2n)^3$ to sustain optical resonance. In this context, the quest to transcend the diffraction limit and usher in a new era of ultra-compact lasers led scientists to explore the intriguing concept of surface plasmons as a replacement for traditional photonic resonance within laser cavities (Jin et al., 2021).

The concept of surface plasmons, which involve collective oscillations of electrons at the interface between a metal and a dielectric material, offered a tantalizing opportunity to circumvent the optical diffraction limit (Deka et al., 2020). In 2009, a groundbreaking achievement by Oulton et al. at UC Berkeley marked a significant milestone in this pursuit with the successful demonstration of the first surface Plasmon Polariton (SPP) nanolasers. (R. Wang et al., 2023) These nanolasers employed CdS nanowires placed atop a silver substrate, augmented with a layer of MgF. The remarkable advantages of these SPP nanolasers included their minuscule size and the dramatic enhancement of localized electromagnetic fields within the active regions of the devices (Gomes et al., 2023).

Building upon this seminal work, further breakthroughs followed, including the creation of scalable plasmonic nanolasers using core-shell semiconductor nanowires on silver substrates. (Xavier et al., 2018) These pioneering achievements fueled an ongoing exploration of novel materials and structures to harness the potential of surface plasmons for achieving lasers with unprecedented miniaturization and performance (Deka et al., 2020).

Amidst this backdrop of scientific innovation, graphene emerged as a material of immense promise. Graphene, a one-atom-thick lattice of carbon atoms arranged in a honeycomb crystal lattice, possesses extraordinary electronic properties. Notably, its carrier mobility can reach values as high as approximately 15.000 $cm^2/V.s$, surpassing that of conventional silicon. (Deka et al., 2020) This exceptional carrier mobility, coupled with its remarkable electrical conductivity and transparency, positioned graphene as a compelling candidate to revolutionize various fields, including semiconductors, electronics, and opto-electronics (Zhou et al., 2019).

Graphene's potential extends to plasmonic lasers as well. In particular, its ultrathin nature and excellent electrical properties make it feasible to introduce a single-layered, sub-nanometer-thick graphene sheet within the Semiconductor-Insulator-Metal (SIM) structure of plasmonic nanolasers. (Ma & Wang, 2021) This strategic incorporation of graphene aims to maintain the critical capability of forming SPPs while simultaneously enabling the modulation of laser performance through the application of externally applied current. This pioneering approach not only facilitates the development of ultra-compact, actively controllable lasers but also opens up exciting prospects for their integration into advanced opto-electronic integrated circuits (R. Wang et al., 2023).

In the ensuing sections, we undertake a comprehensive examination of the experimental results and engage in in-depth discussions. Our aim is to elucidate the substantial influence exerted by graphene on the performance of plasmonic nanolasers, while also elucidating the fundamental mechanisms that underpin these captivating advancements (D. Wang et al., 2018).

The influence of graphene on the performance of plasmonic nanolasers is diverse, contingent on specific design considerations and implementation strategies. When effectively integrated into the metal layer of a plasmonic nanolaser, graphene exhibits advantages such as lower intrinsic material loss compared to conventional metals like silver or gold. This translates into a reduced lasing threshold, enabling the laser to operate at lower pumping power, thereby enhancing energy efficiency. Moreover, the plasmonic properties of the nanolaser become tunable by manipulating the interaction between graphene and the metal layer, achieved through adjusting the Fermi level via external gating or chemical doping. (Hill et al., 2009)This fine-tuning capability extends to resonant wavelength modulation and other key plasmonic characteristics. Additionally, the introduction of graphene in combination with dielectrics facilitates the creation of hybrid plasmonic modes, presenting novel advantages, including improved field confinement and reduced radiation loss. (Schawlow & Townes, 1958) However, it is crucial to acknowledge that challenges, such as fabrication complexities, limited interaction thickness, dependence on graphene quality, dynamic control intricacies, and environmental sensitivity, accompany the integration of graphene into plasmonic nanolasers. Successful harnessing of graphene's potential necessitates careful consideration of these factors, from design and fabrication to control strategies, to optimize performance while addressing inherent limitations (Ma & Wang, 2021).

2. THEORETICAL ANALYSIS

Surface Plasmons (SPs) stand as a unique manifestation of electromagnetic energy waves arising when an external light field strikes the interface between a metal medium. This encounter triggers a reorganization of the free electrons within the metal, leading to a collective oscillatory response. Theoretical scrutiny has illuminated that SPs waves are characterized by their exclusive adherence to the Transverse Magnetic (TM) polarization mode along the metal-medium interface. The dispersion relation for SPs is articulated as follows (Kaliberda & Pogarsky, 2023):

$$k_{sp} = \frac{\omega}{c}\sqrt{\frac{\varepsilon_m \varepsilon_d}{\varepsilon_m + \varepsilon_d}} \qquad (1)$$

Within the given formula, ε_m and ε_d stand for the dielectric constants of the metal and the surrounding medium, respectively, while ω/c represents the wave vector of the incident light within the air. It is noteworthy that the wave vector of the incident light field consistently falls short of the propagating wave vector of Surface Plasmons (SPs), a fundamental attribute of these waves. Employing the phase shift method, Surface Plasmons can be effectively excited only when these two vectors are precisely matched.

Nonetheless, owing to the presence of ohmic loss in the metal, the energy carried by the surface wave diminishes as it traverses longer distances. To quantify this phenomenon, we calculate the propagation length of SPs using the following expression:

$$L_{spp} = \lambda_0 \frac{(\varepsilon_m^{'})^2}{2\pi\varepsilon^{''}} \left(\frac{\varepsilon_m^{'} + \varepsilon_d}{\varepsilon_m^{'} \varepsilon_d} \right)^{\frac{3}{2}} \qquad (2)$$

Here, $\varepsilon_{m'}$ represents the real component of the metal's dielectric constant, while $\varepsilon_{m''}$ denotes its imaginary component. Observing the formula above, it becomes apparent that to achieve an extensive transmission length, the real component of the metal's dielectric constant should be higher, while the imaginary component should be lower. Precious metals are preferred due to their low loss and low absorption coefficient, meeting these conditions. Consequently, precious metals, such as gold and silver, are commonly chosen for this purpose, with silver being a popular choice for metal in various designs, as indicated in references.

3. RESULTS AND DISCUSSIONS

The methodology employed to measure the threshold power for the four structures involved a systematic and controlled experimental procedure. In this study, ZnO nanowires were deposited on each of the four sample configurations, as illustrated in Figure 1. Two of these samples, denoted as case I and case III, featured an additional layer of Al2O3 on the silver casing to mitigate the natural growth of a native oxide layer on aluminum (Al). The remaining two samples, corresponding to case II and case IV, shared identical structures with case I and case III but had graphene transferred onto them. To conduct the threshold power measurements, optical property assessments were carried out at a cryogenic temperature of 77 K using a micro-PhotoLuminescence (μ-PL) system. The excitation source for these experiments was a pulsed laser emitting at 355 nm, characterized by a short pulse width of 0.5 ns and a repetition rate of 1 kHz. This specific experimental setup allowed for precise investigation of the plasmonic nanolasers' behavior.

The threshold power measurements involved gradually increasing the pumping power incident on the nanowire while monitoring the resulting lasing characteristics. The average threshold characteristics for the four structures were then determined and analyzed, providing quantitative insights into how the presence of graphene, additional layers, and variations in metal substrates influenced the lasing threshold. This methodological approach ensured a systematic and comparative assessment of the performance of plasmonic nanolasers with different structural configurations, laying the foundation for a comprehensive understanding of the impact of graphene on the threshold power in these nanoscale laser systems.

To investigate the influence of graphene on the performance of plasmonic nanolasers, four sample structures were fabricated, as illustrated in Figure 1. An additional layer of Al_2O_3 was introduced onto the silver casing for two of these samples, referred to as case I and case III, to mitigate the natural growth of a native oxide layer on aluminum (Al). Graphene was subsequently transferred onto the remaining two samples, corresponding to case II and case IV, which shared identical structures with case I and case III.

ZnO nanowires were deposited on all four samples to serve as gain media for the nanolasers. Optical property measurements were conducted at 77 K using a µ-PL system with a 355 nm N_dYNO_4 pulse laser as the excitation source. The average threshold characteristics of the four structures are shown in Figure 2. Notably, aluminum exhibited a lower average threshold when graphene was present, while silver showed a different trend. This difference can be attributed to variations in the work function of the metals with respect to graphene. The presence of a 5 nm Al_2O_3 layer between graphene and metal led to distinct carrier density distributions, influencing the plasma frequency and, consequently, the propagation length and confinement factor of SPP modes.

Furthermore, we applied external current ranging from 0 mA to 200 mA to the graphene sheet in the ZnO nanowire/graphene/Al template while maintaining a fixed pumping power incident on the nanowire. The lasing peak intensity gradually decreased as the applied current increased, and upon reducing the current back to 0 mA, the lasing peak gradually restored. Figure 3 illustrates the lasing characteristics under different applied currents to graphene. With increasing current, the threshold increased from 80 µW, 150 µW, and 300 µW under 0 mA, 100 mA, and 150 mA applied currents, respectively. Remarkably, lasing ceased under a 200 mA applied current, even with a pumping power of up to 800 µW. This switching modulation behavior can be attributed to the built-in electric field that accelerated charges, inducing additional relaxation channels and consequently raising the damping constant in the Drude-Lorentz model of graphene, resulting in increased threshold levels.

Figure 1 illustrates the schematic representations of the four distinct sample structures employed in our study. These schematics provide a visual overview of the experimental setups, showcasing the unique configurations that were investigated to assess the influence of graphene on plasmonic nanolaser performance.

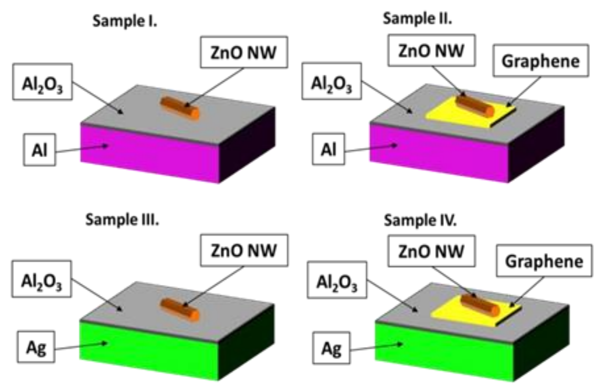

(a)

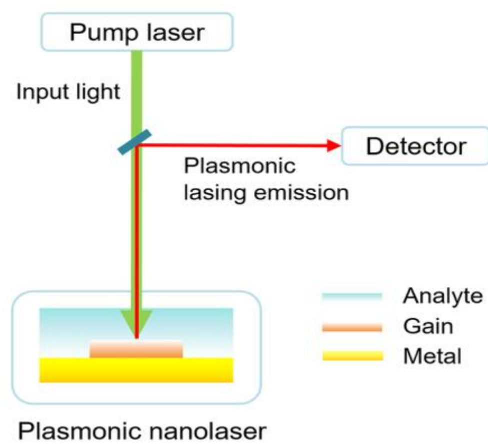

(b)

Figure 1. (a) Schematics of four sample structures; (b) Measurement block diagram

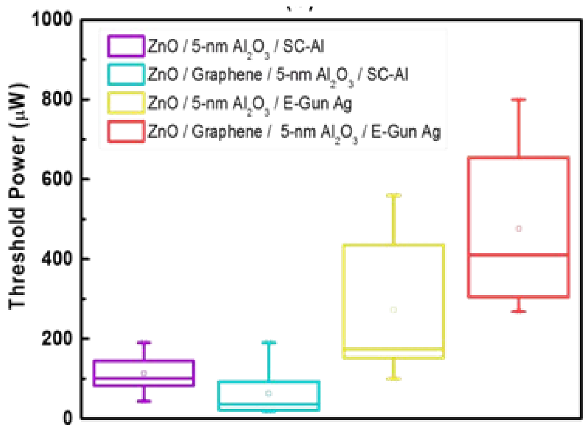

Figure 2. The statistic graph of thresholds from four samples

Figure 3 displays a statistical graph depicting the threshold characteristics obtained from the four distinct samples investigated in our study. This graph provides a quantitative representation of the laser threshold values observed across these samples, offering valuable insights into the impact of graphene on the performance of plasmonic nanolasers.

Following the integration of ZnO nanowires onto all four sample configurations to facilitate gain, we meticulously evaluated the optical properties of these setups. Employing a micro-PhotoLuminescence (μ-PL) system, we conducted these assessments at a cryogenic temperature of 77 K. The excitation source utilized was a pulsed laser emitting at 355 nm, characterized by an exceptionally short pulse width of 0.5 ns and an impressive repetition rate of 1 kHz. This carefully chosen experimental setup enabled us to precisely investigate the plasmonic nanolasers' behavior.

To gain a comprehensive understanding, we conducted threshold characteristic assessments across more than ten individual nanowires for each configuration. The findings from these evaluations were aggregated to calculate the average thresholds, which are graphically depicted in Figure 2.

An intriguing observation emerged when comparing the performance of plasmonic nanolasers on aluminum and silver substrates, specifically concerning the presence of graphene within the structure. In the aluminum case, the average threshold was consistently lower when graphene was introduced compared to configurations without graphene. This noteworthy effect could be attributed to the disparity in work functions between the metals and graphene.

Aluminum (Al), for instance, introduced an abundance of free electrons to graphene, a phenomenon known as n-doping. In contrast, silver (Ag) extracted free electrons from graphene, resulting in p-doping. However, it is essential to emphasize the pivotal role played by a 5 nm layer of Al_2O_3 interposed between graphene and the metal substrate.

This ultra-thin insulating layer served as an intricate mediator, orchestrating the distribution of charge carriers. In the case of aluminum, it led to the preferential allocation of electrons to the graphene side, while in the silver case, it caused a segregation of holes and electrons onto their respective sides of graphene. This unique modulation of carrier distribution had profound implications for the plasma frequency, a fundamental parameter governing the propagation length and confinement factor of SPP modes.

Furthermore, we embarked on an exploration of the dynamic behavior of plasmonic nanolasers in the graphene/aluminum configuration, where ZnO nanowires were integrated. To facilitate active modulation of the nanolasers, we introduced an external current ranging from 0 mA to 200 mA to the graphene sheet, while simultaneously maintaining a constant pumping power incident on the nanowire. This meticulously designed experiment enabled us to delve into the nuanced intricacies of plasmonic nanolaser behavior under varying current conditions.

As the applied current gradually increased from 0 mA to 200 mA, we observed a corresponding decay in the lasing peak intensity. The gradual decline in peak intensity served as a clear indicator of the dynamic modulation capabilities of the plasmonic nanolasers in response to changes in the applied current. Interestingly, upon reverting the applied current back from 200 mA to 0 mA, the lasing peak exhibited a gradual and promising restoration, as visually represented in Figure 3

Figure 4 provided a comprehensive exploration of the lasing characteristics under varying levels of applied current to the graphene layer. As the applied current was progressively increased, there was a noticeable elevation in the lasing threshold. Specifically, the threshold values exhibited an upward trend, increasing from 80 μW to 150 μW, and further to 300 μW, as the current levels escalated from 0 mA to 100 mA, and subsequently to 150 mA, respectively. Remarkably, under the highest applied current of 200 mA, lasing ceased to occur, despite the substantial increase in pumping power to 800 μW.

The underlying mechanism driving this intriguing switching modulation phenomenon was attributed to the presence of the built-in electric field. This electric field induced an acceleration of charge carriers within the graphene structure, subsequently opening up additional relaxation channels. Consequently, these intricate charge dynamics led to a pronounced increase in the damping constant within the Drude-Lorentz model of graphene.

This increase in damping constant was a key factor contributing to the observed elevation in the lasing threshold as the applied current intensified. These empirical findings underscored the remarkable feasibility of actively controlling and modulating plasmonic nanolasers through the application of external current. This breakthrough has profound implications for the development of ultra-compact lasers with dynamic functionality, thereby advancing the frontiers of opto-electronic integrated circuits and their potential applications in cutting-edge technologies.

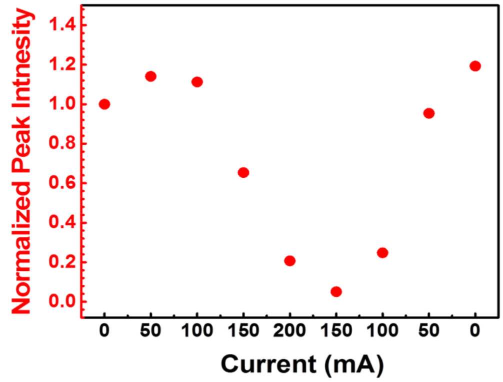

Figure 3. Plot of normalized peak intensity corresponding to different current while the nanowire was optically pumped at 280 uW

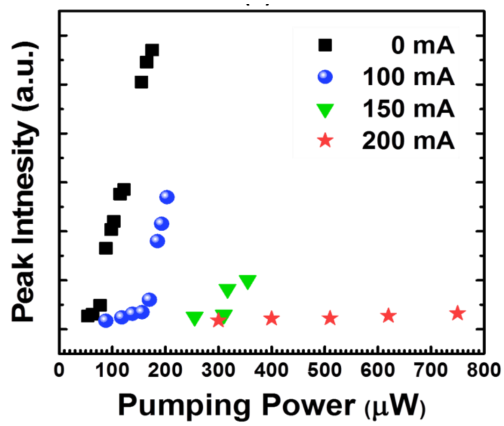

Figure 4. Lasing thresholds under different current when the nanowire was optically pumped with the same power.

4. CONCLUSION

We have successfully fabricated and demonstrated a surface plasmon polariton (SPP) nanolaser device utilizing graphene, which has shown the novel capability of modulation through externally applied current, marking a significant advancement in the field. The incorporation of graphene within the device structure resulted in a notable reduction in the lasing threshold for ZnO nanowires on an aluminum substrate. This observed effect is attributed to alterations in the refractive index of graphene due to the transfer of electrons or holes between graphene and the underlying metal substrate. Furthermore, the nanolaser device employing a ZnO nanowire/graphene/Al_2O_3/Al configuration exhibited the modulation of lasing characteristics by the application of external current to the graphene layer. These findings represent a substantial step forward and open up avenues for the development of actively controllable, ultra-compact lasers with potential applications in opto-electronic integrated circuits.

Our investigation into graphene-based plasmonic nanolasers has unveiled a series of remarkable insights into the modulation and performance of these ultra-compact laser devices. We embarked on a comprehensive exploration of various sample configurations, shedding light on the intricate interplay between graphene, metallic substrates, and external current. The key findings and implications of our study can be summarized as follows:

Optical Properties and Threshold Characteristics: With the integration of ZnO nanowires as gain media, we meticulously evaluated the optical properties of the four distinct sample structures. Our analysis, conducted at a cryogenic temperature of 77 K using a μ-PL system, revealed a pivotal distinction in threshold behavior between aluminum and silver cases when graphene was introduced. Notably, the average threshold was consistently lower in the presence of graphene in the aluminum case, while the silver case exhibited contrasting trends.

Graphene-Metal Interaction: The differences in threshold behavior were attributed to the interaction between graphene and the underlying metal substrates. Aluminum (Al) introduced free electrons to graphene, resulting in n-doping, whereas silver (Ag) extracted free electrons from graphene, leading to p-doping. Crucially, the presence of a 5-nanometer (nm) layer of aluminum oxide (Al_2O_3) between graphene and the metal substrates played a critical role in segregating charge carriers, further influencing threshold characteristics.

Modulation through External Current: In a significant advancement, we demonstrated the dynamic modulation of plasmonic nanolasers by applying external current to the graphene layer. As the applied current increased from 0 mA to 200 mA, a gradual decay in lasing peak intensity was observed. Intriguingly, when the applied current was subsequently reduced from 200 mA back to 0 mA, the lasing peak exhibited a gradual restoration.

Threshold Elevation with Increasing Current: Our comprehensive examination of lasing characteristics under varying levels of applied current revealed a direct correlation between current intensity and threshold elevation. As the applied current escalated, the lasing threshold exhibited an upward trend. Under the highest applied current of 200 mA, lasing ceased despite the substantial increase in pumping power, showcasing the intriguing potential for active modulation.

Mechanism of Modulation: The observed switching modulation phenomenon was attributed to the built-in electric field's influence on charge carriers within the graphene structure. This effect induced additional relaxation channels and led to an increase in the damping constant within the Drude-Lorentz model of graphene. Consequently, the lasing threshold exhibited dynamic behavior in response to changes in applied current.

These findings collectively underscore the remarkable feasibility of actively controlling and modulating plasmonic nanolasers through the application of external current. This breakthrough not only enhances our understanding of the intricate interactions between graphene, metallic substrates, and external stimuli but also opens up exciting prospects for the development of ultra-compact lasers with dynamic functionality.

The implications of this research extend to various domains, including opto-electronic integrated circuits and advanced technologies reliant on compact, actively controllable laser sources. As we continue to explore the potential of graphene-based plasmonic nanolasers, we anticipate further advancements that will contribute to the ever-evolving landscape of photonics and its applications in cutting-edge science and technology

The theoretical outcomes of this study, featuring graphene-based plasmonic nanolasers, hold substantial practical significance across various applications. The integration of graphene introduces benefits such as lower metallic loss, reduced lasing threshold, and tunable plasmonic properties, promising advancements in compact laser sources for opto-electronic integrated circuits. The ability to actively control these nanolasers through external current adds dynamic functionality, making them valuable for telecommunications, sensing technologies, and information processing. Additionally, the study unveils novel hybrid modes with enhanced field confinement and reduced radiation loss, indicating potential applications in advanced sensing and high-performance computing. The theoretical results not only contribute to nanophotonics but also pave the way for transformative technologies with wide-ranging practical implications.

REFERENCES

Deka, S. S., Jiang, S., Pan, S. H., & Fainman, Y. (2020). Nanolaser arrays: Toward application-driven dense integration. *Nanophotonics*, *10*(1), 149–169. https://doi.org/10.1515/nanoph-2020-0372

Gomes, A. S. L., Menezes, L. D. S., & De Oliveira, H. P. (2023). Nanophotonics in modern plasmonics and nanolasers. In *Modern Luminescence from Fundamental Concepts to Materials and Applications* (pp. 275–312). Elsevier. https://doi.org/10.1016/B978-0-323-89954-3.00004-1

Hill, M. T., Marell, M., Leong, E. S. P., Smalbrugge, B., Zhu, Y., Sun, M., Van Veldhoven, P. J., Geluk, E. J., Karouta, F., Oei, Y.-S., Nötzel, R., Ning, C.-Z., & Smit, M. K. (2009). Lasing in metal-insulator-metal sub-wavelength plasmonic waveguides. *Optics Express*, *17*(13), 11107. https://doi.org/10.1364/OE.17.011107

Jin, Y., Zhou, L., Liang, J., & Zhu, J. (2021). Electrochemically driven dynamic plasmonics. *Advanced Photonics*, *3*(04). https://doi.org/10.1117/1.AP.3.4.044002

Kaliberda, M. E., & Pogarsky, S. A. (2023). Tunability of Radiation Pattern of the H-Polarized Natural Waves of Dielectric Waveguide with Infinite Graphene Plane and Finite Number of Graphene Strips at THz. *Applied Sciences*, *13*(19), 10563. https://doi.org/10.3390/app131910563

Ma, R.-M., & Wang, S.-Y. (2021). Plasmonic nanolasers: Fundamental properties and applications. *Nanophotonics*, *10*(14), 3623–3633. https://doi.org/10.1515/nanoph-2021-0298

Schawlow, A. L., & Townes, C. H. (1958). Infrared and Optical Masers. *Physical Review*, *112*(6), 1940–1949. https://doi.org/10.1103/PhysRev.112.1940

Wang, D., Wang, W., Knudson, M. P., Schatz, G. C., & Odom, T. W. (2018). Structural Engineering in Plasmon Nanolasers. *Chemical Reviews*, *118*(6), 2865–2881. https://doi.org/10.1021/acs.chemrev.7b00424

Wang, R., Wang, C., Ma, Y., Sun, J., Yan, P., Xu, C., & Pan, C. (2023). Recent Progress in Low Threshold Plasmonic Nanolasers. *Advanced Optical Materials*, *11*(15), 2203137. https://doi.org/10.1002/adom.202203137

Xavier, J., Vincent, S., Meder, F., & Vollmer, F. (2018). Advances in optoplasmonic sensors – combining optical nano/microcavities and photonic crystals with plasmonic nanostructures and nanoparticles. *Nanophotonics*, *7*(1), 1–38. https://doi.org/10.1515/nanoph-2017-0064

Zhou, Z.-K., Liu, J., Bao, Y., Wu, L., Png, C. E., Wang, X.-H., & Qiu, C.-W. (2019). Quantum plasmonics get applied. *Progress in Quantum Electronics*, *65*, 1–20. https://doi.org/10.1016/j.pquantelec.2019.04.002

ĐIỀU KHIỂN ĐỘNG HỌC CỦA GRAPHIT - KÍCH HOẠT TIA LASER NANO PLASMONIC

Hồ Xuân Trường[1*]

[1]*Trường Đại học Công nghệ Đồng Nai*

*Tác giả liên hệ: *Hồ Xuân Trường, hoxuantruong@dntu.edu.vn*

THÔNG TIN CHUNG

Ngày nhận bài: 30/12/2023

Ngày nhận bài sửa: 05/02/2024

Ngày duyệt đăng: 12/03/2024

TỪ KHOÁ

Sự điều biến graphit;
Tia laser thu nhỏ;
Quang điện tử tích hợp;
Máy phát laser nano Plasmonic;
Phân cực bề mặt Plasmon.

TÓM TẮT

Trong nghiên cứu này, tác giả trình bày kết quả nghiên cứu về máy phát laser nano sử dụng graphit làm thành phần cơ bản của nó. Máy laser nano này thể hiện một tính năng đặc biệt đó là khả năng điều chỉnh hoạt động thông qua dòng điện tác dụng bên ngoài đồng thời điều chỉnh được cường độ ánh sáng quang học. Các thí nghiệm bao gồm đánh giá sự cải tiến của việc chuyển đổi hiệu suất bật và tắt tia laser nano plasmonic, và đây là một nghiên cứu mới và quan trọng trong lĩnh vực quang tử nano. Sử dụng graphit trong khung cấu trúc của máy laser nano là ứng dụng khả năng di chuyển đặc biệt của vật liệu này và các đặc tính quang điện đáng chú ý của nó. Chính đặc điểm này đã giúp graphit trở thành một vật liệu tốt phù hợp cho sự tích hợp vào các mạch quang điện tử. Nghiên cứu này trình bày một cách đầy đủ về các kết quả thực nghiệm, qua đó làm sáng tỏ ảnh hưởng sâu sắc của graphit đến hiệu suất của máy phát laser nano plasmonic cũng như nghiên cứu sâu vào các vấn đề về kết cấu của graphit.